

Coherent optical nano-tweezers for ultra-cold atoms

P. Bienias,^{1,*} S. Subhankar,¹ Y. Wang,¹ T-C Tsui,¹ F. Jendrzejewski,² T. Tiecke,^{3,†}
G. Juzeliūnas,⁴ L. Jiang,^{5,6} S. L. Rolston,¹ J. V. Porto,¹ and A. V. Gorshkov^{1,7}

¹*Joint Quantum Institute, NIST/University of Maryland, College Park, Maryland 20742 USA*

²*Kirchhoff Institut für Physik, Universität Heidelberg,
Im Neuenheimer Feld 227, 69120 Heidelberg, Germany*

³*Department of Physics, Harvard University, Cambridge, Massachusetts 02138, USA*

⁴*Institute of Theoretical Physics and Astronomy, Vilnius University,
Saulėtekio Avenue 3, LT-10257 Vilnius, Lithuania*

⁵*Department of Applied Physics, Yale University, New Haven, Connecticut 06520, USA*

⁶*Yale Quantum Institute, Yale University, New Haven, Connecticut 06511, USA*

⁷*Joint Center for Quantum Information and Computer Science,
NIST/University of Maryland, College Park, Maryland 20742 USA*

There has been a recent surge of interest and progress in creating subwavelength free-space optical potentials for ultra-cold atoms. A key open question is whether geometric potentials, which are repulsive and ubiquitous in the creation of subwavelength free-space potentials, forbid the creation of narrow traps with long lifetimes. Here, we show that it is possible to create such traps. We propose two schemes for realizing subwavelength traps and demonstrate their superiority over existing proposals. We analyze the lifetime of atoms in such traps and show that long-lived bound states are possible. This work opens a new frontier for the subwavelength control and manipulation of ultracold matter, with applications in quantum chemistry and quantum simulation.

Coherent manipulation of atoms using light is at the heart of cold-atom-based quantum technologies such as quantum information processing and quantum simulation [1, 2]. The most commonly used methods to trap atoms optically are based on the AC Stark shift induced in a two-level system by an off-resonant laser field, which provides a conservative potential that is proportional to laser intensity. The spatial resolution of such a trapping potential is diffraction-limited, unless operated near surfaces [3–8]. In contrast, a three-level system with two coupling fields offers more flexibility and can generate a subwavelength optical potential even in the far-field: although the intensity profiles of both laser beams involved are diffraction-limited, the internal structure of the state can change in space on length scales much shorter than the wavelength λ of the lasers [9–18]. Such subwavelength internal-state structure can lead to subwavelength potentials either by creating spatially varying sensitivity to a standard AC Stark shift [19] or by inducing a conservative subwavelength geometric potential [20–22].

Trapping atoms in the far field on the subwavelength scale may allow for the realization of Hubbard-type models with increased tunneling and interaction energies [3, 7, 8, 23, 24], which in turn would relax requirements on the temperature and coherence times in such experiments. Subwavelength traps can also be useful in atom-based approaches to quantum information processing [25, 26] and quantum materials engineering, as well as for efficient loading into traps close to surfaces [3–8]. The use of dynamically adjustable subwavelength tweezers [27, 28], in which atoms can be brought together and apart, can also enable controlled ultracold quantum chemistry [29–31].

To trap atoms on a subwavelength scale, the optical potential must provide a local minimum. The geometric scalar potential associated with laser-induced internal-state structure is always repulsive and increases in magnitude as its spatial extent is reduced. This repulsive contribution must be considered when engineering attractive subwavelength optical potentials. A trap based on the combination of AC Stark shift and subwavelength localization [9–16, 32–52] within a three-level system was proposed in Ref. [19], but the geometric potentials arising from non-adiabatic corrections to the Born-Oppenheimer approximation [20, 21] were not considered. In this Letter, we show that even with the repulsive non-adiabatic corrections, attractive subwavelength potentials are still possible. We also propose two alternative schemes for the generation of traps that offer significantly longer trapping times as compared to the approach of Ref. [19]. We analyze the performance of all three approaches and show that 8nm-wide traps offering 10ms trapping times are within reach. Compared with near-field methods, our far-field approach not only avoids losses and decoherence mechanisms associated with proximity to surfaces, but also provides more flexibility in time-dependent control of the shape and position of the trapping potentials and, additionally, works not only in one and two but also in three dimensions.

Model.—We start with a single-atom Hamiltonian

$$H = H_{\text{al}}(x) + \frac{p^2}{2m}, \quad (1)$$

where m is the mass, p is the momentum, and H_{al} describes the atom-light interaction. We will consider three schemes shown in Fig. 1: (a) electromagnetically induced transparency (EIT), (b) blue-detuned AC-Stark, and (c)

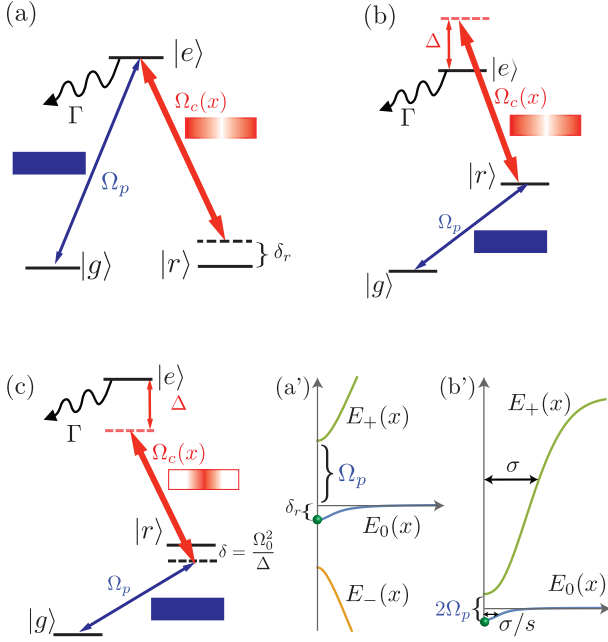


FIG. 1. (a) Level diagram for the EIT scheme, showing a spatially homogeneous field Ω_p [blue bar] and a spatially varying field $\Omega_c(x) = \Omega_0(1 - e^{-x^2/\sigma^2})^{1/2}$ [red bar with gradient]. Γ is the linewidth of the excited state. (b) Level diagram for the blue-detuned AC-Stark scheme. The intermediate state $|r\rangle$ is dressed by coupling it to the excited state $|e\rangle$ with a spatially dependent $\Omega_c(x) = \Omega_0(1 - e^{-x^2/\sigma^2})^{1/2}$ and a large detuning $\Delta \gg \Omega_c$, which gives rise to a light-shift $\Omega_c^2(x)/\Delta$ of state $|r\rangle$. The ground state $|g\rangle$ is coupled to state $|r\rangle$ with a spatially uniform Ω_p and detuning $\delta = 0$. (c) Level diagram for the red-detuned AC-Stark scheme [19]. The difference from (b) is that $\Omega_c(x) = \Omega_0 e^{-x^2/(2\sigma^2)}$ is maximal at $x = 0$ and that $|\Delta| \gg \Omega_c$, δ now indicates the amount of red detuning. Moreover, the detuning $\delta = \Omega_0^2/\Delta$ is chosen to exactly compensate for the light-shift of $|r\rangle$ at $x = 0$. (a',b') Sketches of the relevant eigenstates (atom depicted by a green ball is trapped in the blue potential): (a') for the (a) scheme; (b') for the (b) scheme, which for $x < w$ is equivalent to the (c) scheme. Although E_{\pm} are diffraction limited, E_0 has subwavelength shape characterized by width w , which can be expressed using the enhancement factor defined as $s = \sigma/w$.

red-detuned AC-Stark [19]. For the EIT scheme ($\hbar = 1$),

$$H_{\text{al}} = \begin{pmatrix} \delta_r & 0 & \Omega_c(x) \\ 0 & 0 & \Omega_p \\ \Omega_c(x) & \Omega_p & \Delta \end{pmatrix} \quad (2)$$

in the basis of bare atomic states $\{|r\rangle, |g\rangle, |e\rangle\}$, where $2\Omega_p$ and $2\Omega_c(x)$ are Rabi frequencies of a spatially homogeneous probe field and a spatially-varying control field, respectively. For the two AC-Stark schemes, in the limit of large single-photon detuning $|\Delta| \gg \Omega_c(x), \Omega_p, |\delta|$ [see Fig. 1(b,c)], the intermediate state $|e\rangle$ can be adiabatically eliminated, resulting in an effective two-state

Hamiltonian

$$H_{\text{al}} = \begin{pmatrix} \delta - \frac{\Omega_c^2(x)}{\Delta} & \Omega_p \\ \Omega_p & 0 \end{pmatrix} \quad (3)$$

in the $\{|r\rangle, |g\rangle\}$ basis.

Within the Born-Oppenheimer approximation, we first diagonalize H_{al} which leads to position-dependent eigenstates. Non-adiabatic corrections give rise to geometric scalar U and vector A potentials, defined as $U = R^\dagger \partial_x^2 R$ and $A = iR^\dagger \partial_x R$, where R is a unitary operator diagonalizing H_{al} [20, 21]. The resulting Hamiltonian is given by $H' = R^\dagger H R = R^\dagger H_{\text{al}} R + U(x) + \frac{p^2}{2m} - \frac{A(x)p}{m}$. Below, we focus on the potential $R^\dagger H_{\text{al}} R + U(x)$ experienced by three-level atoms under three different schemes.

EIT scheme.—In Refs. [20–22], subwavelength barriers were considered in the EIT configuration assuming two-photon resonance, i.e. $\delta_r = 0$ in Fig. 1(a). The approximate dark state $|D\rangle \propto \Omega_c(x)|g\rangle - \Omega_p|r\rangle$ then experiences only a repulsive geometric potential $\langle D|U|D\rangle$. On the other hand, in the presence of a finite detuning δ_r for state $|r\rangle$, the dark state $|D\rangle$ can acquire a negative energy shift $E_0(x)$ with an absolute value greater than the positive geometric potential. Moreover, we see that, as we move from large to small x , the state $|D\rangle$ changes its character from $|g\rangle$ to $|r\rangle$ at $x = w$ defined via $\Omega_c(w) = \Omega_p$. Therefore, for $\Omega_0 \gg \Omega_p$, we can engineer subwavelength traps with width $w \ll \sigma$. However, at first glance, it is not obvious whether the additional contribution from the repulsive geometric potential would cancel the attractive potential. Moreover, the approximate dark state experiencing the trapping potential can have a significant admixture of state $|e\rangle$, leading to loss. Below, we address these two issues.

In the following, for simplicity, we set $\Delta = 0$ because, for a single trap in the EIT configuration, nearly all results (except the tunneling losses to the lower dressed-state $|-\rangle$) are Δ -independent. For $|\delta_r + U(x)| \ll \Omega_p$, the bright states $|\pm\rangle$ are well-separated from the dark state. In this case, the ground state is composed of the dark state with a small admixture of bright states, so that the geometric potential and the energy shift E_0 can be calculated separately, see Fig. 1(a'). Note that, for all schemes, we will take into account decay Γ of state $|e\rangle$ perturbatively. We are interested in a spatially dependent [53] control Rabi frequency $\Omega_c(x) = \Omega_0(1 - e^{-x^2/\sigma^2})^{1/2}$. For small x , $\Omega_c \approx \Omega_0 x/\sigma$, so that the total effective potential $V_{\text{tot}} = |\langle D|r\rangle|^2 \delta_r + U_D$ is equal to

$$V_{\text{tot}} = \frac{\delta_r}{1 + x^2/w^2} + \frac{1}{2mw^2} \frac{1}{(1 + x^2/w^2)^2}, \quad (4)$$

where we used $U_D = \langle D|U|D\rangle = \frac{1}{2m} \left(\frac{\Omega_p \partial_x \Omega_c(x)}{\Omega_p^2 + \Omega_c^2(x)} \right)^2$ and $w = \sigma \Omega_p / \Omega_0$. We see explicitly that the trapping potential has subwavelength width w , which can be characterized by the enhancement factor $s = \sigma/w$, and that U_D is always repulsive.

To compare all three schemes, we start by considering traps that have a specific width w and support a single bound state. Furthermore, we assume that our maximum Rabi frequency $\Omega_c(x)$ is limited to Ω_0 . In that case, if we drop factors of order unity, our scheme supports a single bound state when the kinetic energy $E_w = 1/(2mw^2)$ is equal the depth of the potential V_{tot} .

The leading source of loss comes from the admixture of the short-lived state $|e\rangle$. There are two processes leading to this admixture: (1) imperfect EIT due to $\delta_r \neq 0$ and (2) non-adiabatic off-diagonal corrections. Both processes admix $|D\rangle$ with $|\pm\rangle$, which in turn have significant overlap with $|e\rangle$. Within second-order perturbation theory, the loss rates from processes (1) and (2) are $\Gamma_D^{(1)} \sim \Gamma V_{\text{tot}}^2/\Omega_p^2$ and $\Gamma_D^{(2)} \sim \Gamma \frac{U_{D\pm}}{\Omega_p^2} \sim \Gamma \frac{E_w^2}{\Omega_p^2}$, respectively. Here $U_{D\pm} = \langle D|U|\pm\rangle$ and we used the fact that, for a trap with a single bound state, the off-diagonal [21] terms of U are of the same order as E_w . Thus, up to factors of order unity, the total losses are $\Gamma_D \sim \Gamma_D^{(1)} + \Gamma_D^{(2)} \sim \Gamma E_w^2/\Omega_p^2$. We would like to note that we can modify the EIT setup so that non-adiabatic corrections are further suppressed [54] and the only (and unavoidable) losses come from imperfect EIT. The decay rate for the bound state can be expressed using E_σ , Ω_0 , and s as $\Gamma_D \sim \Gamma s^6 (E_\sigma/\Omega_0)^2$, where $E_\sigma \sim 1/(2m\sigma^2)$. An additional constraint on available widths w comes from the fact that our perturbative analysis holds only for $|V_{\text{tot}}|$ and E_w much smaller than the gap to the bright states $|\pm\rangle$, leading to $E_w \ll \Omega_p$, which is equivalent to $s^3 \ll \Omega_0/E_\sigma$. Another source of losses is tunneling from the subwavelength-trapped state [23] to state $|-\rangle$, which, based on a Landau-Zener like estimate [54], is negligible for $s^3 \ll \Omega_0/E_\sigma$. The specific experimental parameters will be analyzed after the presentation of all three schemes.

Blue-detuned AC-Stark scheme.—The second new schemes we propose is shown in Fig. 1(b) and is described by the Hamiltonian (3) with $\delta = 0$. Here, the intermediate state $|r\rangle$ is dressed by coupling it to the excited state $|e\rangle$ with a spatially dependent Rabi frequency $\Omega_c(x) = \Omega_0(1 - e^{-x^2/\sigma^2})^{1/2}$. Together with a large blue detuning $|\Delta| \gg \Omega_c(x)$, this leads to a light-shift $\Omega_c^2(x)/\Delta$ of state $|r\rangle$. At large x , state $|0\rangle$ is equal to $|g\rangle$; whereas, at $x = 0$, it is proportional to $|g\rangle - |r\rangle$. The light-shift E_0 describing the trapped state $|0\rangle$ is equal to

$$E_0(x) = \Omega_p \left(\frac{1}{2} \left(\frac{x}{w} \right)^2 - \sqrt{1 + \frac{1}{4} \left(\frac{x}{w} \right)^4} \right), \quad (5)$$

where the width w equals σ/s with

$$s = \sqrt{\frac{\Omega_0^2}{|\Delta|\Omega_p}}. \quad (6)$$

Intuitively, the width w is equal to the distance at which the AC-stark shift is equal to the coupling Ω_p .

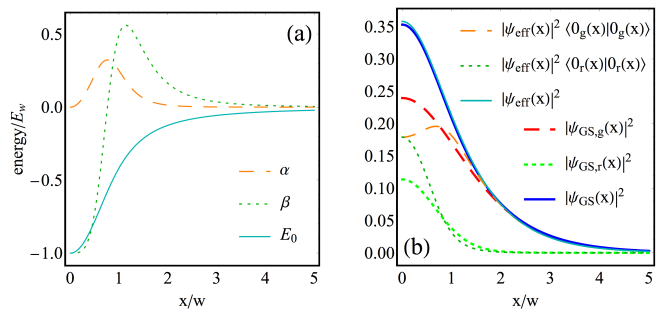


FIG. 2. Analysis of the blue-detuned AC-Stark scheme [Fig. 1(b)]. (a) The light-shift $E_0(x)$, as well as the diagonal and off-diagonal couplings coming from the non-adiabatic potential U in Eq. (7) parametrized by α and β . (b) Properties of the ground state obtained from the effective Hamiltonian and from the full Hamiltonian (see main text for details). Figures are shown in units of w and E_w making them applicable to all $s \gg 1$.

For this scheme, non-adiabatic potential U is equal to

$$U = \begin{pmatrix} \alpha & -\beta \\ \beta & \alpha \end{pmatrix} \quad (7)$$

with $\alpha = E_w \frac{4w^2x^2}{(4w^4+x^4)^2}$ and $\beta = E_w \frac{6x^4-8w^4}{(4w^4+x^4)^2}$. Note that the off-diagonal terms are significantly greater than the diagonal ones (i.e., $\alpha < |\beta|$), especially for $x \lesssim w$, as shown in Fig. 2(a). For $\Omega_p = E_w$, which leads to a single bound state, we obtain β on the order of the energy $E_0(x)$. Note that our derivation works for arbitrary fractional probabilities $f_r = |\psi_r(x)/\psi(x)|$, whereas the method in Ref. [19] works only for fractional probabilities $f_r \ll 1$, where $\psi_r = \langle r|\psi\rangle$ is the r -component of the ground-state wave function ψ .

In order to analyze the impact of U , we compare the ground-state of the effective Hamiltonian $H_{\text{eff}} = E_0(x) - \frac{\partial^2}{2m}$ without U with the exact solution of the full Hamiltonian given by Eqs. (1) and (3). Even though $|\langle 0|U|+\rangle| \sim E_w \sim \Omega_p$ is large and on the order of the energy difference $E_+ - E_0 \sim \Omega_p$, we see in Fig. 2(b) that the probability densities (and therefore the widths) of the ground states ψ_{eff} of H_{eff} and ψ_{GS} of the full Hamiltonian are nearly the same. However, from the comparison of components $|g\rangle$ and $|r\rangle$ of the ground state in Fig. 2(b), we see that the trapped atoms are not exactly in the eigenstate $|0\rangle$. This partially explains why the non-adiabatic corrections do not influence the width of the ground state: the components of the true ground state are smoother (spatial gradients are smaller) than those of the ground state $|0\rangle$ of H_{al} , which leads to weaker non-adiabatic corrections for the true ground state. In summary, even though the non-adiabatic potential U can be on the order of E_w for subwavelength traps, the width of the ground state is only very weakly influenced by U .

We now turn to the analysis of the trap lifetime. The

leading contribution to losses comes from the admixture P_e of the short-lived state $|e\rangle$. P_e is determined by the characteristic coupling strength $\Omega_c(w) \approx \Omega_0/s$ within the trapped region and by the detuning Δ as $P_e \sim (\Omega_0/(\Delta s))^2 \sim s^6(E_\sigma/\Omega_0)^2$. In principle, the condition $\Delta > \Omega_0$ might give an upper limit on s , which, based on Eq. (6), for $\Omega_p = E_w$, is $s^4 < \Omega_0/E_\sigma$. However, this is not a constraint for any of the results considered in this Letter.

Red-detuned AC-Stark scheme.—Finally, we analyze the third scheme, which was proposed in Ref. [19]. Our analysis, compared to the original one, takes into account non-adiabatic corrections and works for arbitrary fractional probabilities. This scheme differs from the blue-detuned AC-Stark scheme in that: first, the control Rabi frequency is $\Omega_c(x) = \Omega_0 e^{-x^2/(2\sigma^2)}$ which, for small x , is $\approx \Omega_0(1 - x^2/(2\sigma^2))$; second, the detuning $\delta = \Omega_0^2/\Delta$ is chosen to exactly compensate for the AC-Stark shift at the center of the trap [55]; third, the detuning Δ now indicates the amount of red detuning. The resulting $E_0 w$, and s are identical to those in the blue-detuned AC-Stark scheme, Eqs. (5) and (6). We find that, for $x \lesssim w$, the non-adiabatic corrections have nearly exactly the same form as in the blue-detuned AC-Stark scheme and differ only in the sign of the off-diagonal terms: $U = \begin{pmatrix} \alpha & \beta \\ -\beta & \alpha \end{pmatrix}$.

To derive the lifetime of this trap, we can set $\Omega_c(x)$ to Ω_0 within the trapped region, which leads to $P_e \sim (\Omega_0^2/\Delta^2) = (s^2\Omega_p/\Omega_0)^2 = s^8(E_\sigma/\Omega_0)^2$. This expression is identical to the one in the EIT and blue-detuned AC-Stark schemes, except for the more favorable scaling with s in our two schemes (s^6 vs. s^8), making them superior. The intuition behind the difference between the two schemes based on the AC-Stark shift is the following: in the red-detuned AC-Stark scheme, the atoms are trapped in the region of maximal scattering from state $|e\rangle$, whereas, in our blue-detuned AC-Stark scheme, atoms are trapped in the region of minimal scattering from state $|e\rangle$.

Atomic levels.—The level structure needed for the two AC-Stark schemes is most easily achieved with alkaline-earth atoms, in which $|g\rangle$, $|r\rangle$, and $|e\rangle$ are chosen to be the ground state 1S_0 , the metastable state 3P_2 , and the state 3D_2 , respectively [56], see Fig. 3(a). The optical separation between the two long-lived states allows the decoupling of Ω_c from $|g\rangle$ to be a much better approximation [57] than what is possible in alkali atoms, where the size of Δ is limited by the fine structure splitting between the D1 and D2 lines [19].

Turning now to the EIT scheme, the subwavelength trap depths achievable with the atomic levels used for barriers in Ref. [58] are limited due to the off-resonant Ω_c -induced coupling of $|g\rangle$ to $|^3P_1, F = 3/2\rangle$ [59], which is detuned by $\Delta_{\text{hfs}}/2\pi = 5.94\text{GHz}$ from $|^3P_1, F = 1/2\rangle$. This coupling gives rise to a position-dependent light-

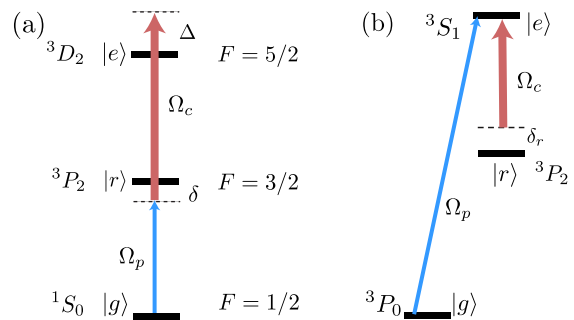


FIG. 3. (a) Atomic levels for the two AC-Stark schemes. The decay rate from the metastable state 3P_2 is negligible ($\Gamma_{3P_2}/2\pi = 0.02\text{Hz}$). (b) Atomic levels for the EIT scheme. In all schemes, the main limitation comes from the admixture of levels outside the 3-level system.

shift of $|g\rangle$ and leads to an additional constraint $\Omega_c \ll \sqrt{\Delta_{\text{hfs}} E_w}$ for trap realization. A solution [similar to the one used for the two AC-Stark schemes] is to protect our three-level system by an optical separation, as shown in Fig. 3(b) [60].

Note that the atomic level configurations in Fig. 3 do not rely on optical polarization selection rules. Therefore, unlike the level configuration of Ref. [22], such subwavelength traps can be extended into 3D.

Achievable trap parameters.—We showed above that, for fixed Ω_0 , the two schemes proposed in this Letter provide superior performance to the red-detuned AC-Stark scheme due to the s^6 vs. s^8 scaling of the losses. We now discuss what widths of the trapping potentials are achievable when we include fundamental limitations imposed on the magnitude of Ω_0 . We set the trapping time T to be equal [3] to 10ms, and consider ^{171}Yb . Depending on the scheme and on σ [equal to $\lambda/2\pi$ for the lattice, and to $3\mu\text{m}$ for the tweezer; denoted by subscripts λ and $3\mu\text{m}$, respectively], we find maximal Ω_0 and s such that the off-resonant position-dependent light-shifts are less than $0.1E_w$ and that $TP_e \sim 1$:

setup	$\frac{\Omega_{0,\lambda}}{2\pi\text{GHz}}$	$\frac{w_\lambda}{\text{nm}}$	s_λ	$\frac{\Omega_{0,3\mu\text{m}}}{2\pi\text{GHz}}$	$\frac{w_{3\mu\text{m}}}{\text{nm}}$	$s_{3\mu\text{m}}$
EIT	13	7.8	16.	2.6	39.	78.
blue-ac	4.1	8.8	36.	1.3	27.	111.
red-ac	1.2	29.	11.	0.28	130.	23.

We see that the EIT and the blue-detuned AC-Stark schemes allow for greater Ω_0 , which translates into narrower traps. For comparison, alkali-atom-based EIT [22] and red-detuned AC-Stark [19] schemes are limited to $\Omega_{0,\lambda}/2\pi = 400\text{MHz}$ (leading to $s = 10$) and $\Omega_{0,\lambda}/2\pi = 150\text{MHz}$ (leading to $s = 1.7$), respectively.

Applications.—We now make a few remarks related to the applications pointed out in the introduction. Note that, if one's goal is simply to use the expansion of a control field $\Omega_c(x)$ around its nodes to create traps with tight bound states with minimal scattering, then our EIT scheme has no advantages over a simple two-level blue-

detuned trap. Indeed, in our case, up to an additive constant, the potential near a node is given by $V(x) \approx \delta_r \Omega_c(x)^2 / \Omega_p^2$, while the population of the excited state is given by $P_e(x) \approx \delta_r^2 \Omega_c^2(x) / \Omega_p^4$. On the other hand, if one uses the same field $\Omega_c(x)$ to create a simple two-level blue-detuned trap (with detuning Δ), one obtains $V(x) \approx \Omega_c^2(x) / \Delta$ and $P_e(x) \approx \Omega_c^2(x) / \Delta^2$. In other words, our scheme is identical to the two-level scheme provided one replaces Δ with Ω_p^2 / δ_r .

However, our goal is not only to create a tight bound state in a trap of subwavelength width w but also to make the trapping potential nearly constant for $|x| > w$ so that we can make and possibly independently move several traps, or a full lattice of traps, with subwavelength separations. In that case, a simple two-level scheme will not work. Instead, one has to use one of the subwavelength schemes we discuss in this Letter.

In combination with stroboscopic techniques [61] or multi-level atomic schemes [20], our traps can lead to the creation of lattices with subwavelength periods, giving rise to large energy scales in Hubbard models [1, 62–65] and in dipolar atomic [66–68] and molecular [69–77] systems, with applications to quantum simulation and quantum computing. Movable subwavelength traps with subwavelength separation may also find applications in ultracold chemistry [29–31].

ACKNOWLEDGMENTS

We are particularly grateful to Misha Lukin and Peter Zoller for stimulating discussions. We also thank Mikhail Baranov, Tommaso Calarco, Gretchen Campbell, Steve Eckel, Mateusz Łacki, Mingwu Lu, Jeff Thompson for helpful discussions. Y.W., S.S., T-C. T., J.V.P., and S.L.R. acknowledge support by NSF PFC at JQI and ONR grant N000141712411. P.B. and A.V.G. acknowledge support by NSF PFC at JQI, AFOSR, ARL CDQI, ARO, ARO MURI, and NSF Ideas Lab. L.J. acknowledges support by ARL CDQI, ARO MURI, Sloan Foundation, and Packard Foundation. F. J. acknowledges support by the DFG Collaborative Research Center ‘SFB 1225 (ISOQUANT)’, the DFG (Project-ID 377616843), the Excellence Initiative of the German federal government and the state governments—funding line Institutional Strategy (Zukunftskonzept): DFG project number ZUK49/Ü.

* bienias@umd.edu

† Present address: Facebook, Inc. 1 Hacker Way, Menlo Park, CA, 94025

[1] C. Gross and I. Bloch, *Science* **357**, 995 (2017).

- [2] M. Lewenstein, A. Sanpera, and V. Ahufinger, *Ultracold Atoms in Optical Lattices: Simulating quantum many-body systems* ("Oxford University Press", 2012).
- [3] A. González-Tudela, C. L. Hung, D. E. Chang, J. I. Cirac, and H. J. Kimble, *Nat. Photonics* **9**, 320 (2015).
- [4] R. Mitsch, C. Sayrin, B. Albrecht, P. Schneeweiss, and A. Rauschenbeutel, *Nat. Commun.* **5**, 5713 (2014).
- [5] J. D. Thompson, T. G. Tiecke, N. P. de Leon, J. Feist, A. V. Akimov, M. Gullans, A. S. Zibrov, V. Vuletić, and M. D. Lukin, *Science* **340**, 1202 (2013).
- [6] D. E. Chang, J. D. Thompson, H. Park, V. Vuletić, A. S. Zibrov, P. Zoller, and M. D. Lukin, *Phys. Rev. Lett.* **103**, 123004 (2009).
- [7] M. Gullans, T. G. Tiecke, D. E. Chang, J. Feist, J. D. Thompson, J. I. Cirac, P. Zoller, and M. D. Lukin, *Phys. Rev. Lett.* **109**, 235309 (2012).
- [8] O. Romero-Isart, C. Navau, A. Sanchez, P. Zoller, and J. I. Cirac, *Phys. Rev. Lett.* **111**, 145304 (2013).
- [9] G. S. Agarwal and K. T. Kapale, *J. Phys. B At. Mol. Opt. Phys.* **39**, 3437 (2006).
- [10] M. Bajcsy, A. S. Zibrov, and M. D. Lukin, *Nature* **426**, 638 (2003).
- [11] Z. Dutton, M. Budde, C. Slowe, and L. V. Hau, *Nature* **293**, 663 (2001).
- [12] A. V. Gorshkov, L. Jiang, M. Greiner, P. Zoller, and M. D. Lukin, *Phys. Rev. Lett.* **100**, 093005 (2008).
- [13] G. Juzeliunas, *Lith. J. Phys.* **47**, 351 (2007).
- [14] J. A. Miles, Z. J. Simmons, and D. D. Yavuz, *Phys. Rev. X* **3**, 031014 (2013).
- [15] M. Sahrhai, H. Tajalli, K. T. Kapale, and M. S. Zubairy, *Phys. Rev. A* **72**, 013820 (2005).
- [16] D. D. Yavuz and N. A. Proite, *Phys. Rev. A* **76**, 041802(R) (2007).
- [17] S. Subhankar, Y. Wang, S. L. Rolston, and J. V. Porto, arXiv:1807.02871v1 (2018).
- [18] M. McDonald, J. Trisnadi, K.-X. Yao, and C. Chin, arXiv:1807.02906v1 (2018).
- [19] D. D. Yavuz, N. A. Proite, and J. T. Green, *Phys. Rev. A* **79**, 055401 (2009).
- [20] M. Łacki, M. A. Baranov, H. Pichler, and P. Zoller, *Phys. Rev. Lett.* **117**, 233001 (2016).
- [21] F. Jendrzejewski, S. Eckel, T. G. Tiecke, G. Juzeliunas, G. K. Campbell, L. Jiang, and A. V. Gorshkov, *Phys. Rev. A* **94**, 063422 (2016).
- [22] Y. Wang, S. Subhankar, P. Bienias, M. Łacki, T. C. Tsui, M. A. Baranov, A. V. Gorshkov, P. Zoller, J. V. Porto, and S. L. Rolston, *Phys. Rev. Lett.* **120**, 083601 (2018).
- [23] W. Yi, A. J. Daley, G. Pupillo, and P. Zoller, *New J. Phys.* **10**, 073015 (2008).
- [24] N. Lundblad, P. J. Lee, I. B. Spielman, B. L. Brown, W. D. Phillips, and J. V. Porto, *Phys. Rev. Lett.* **100**, 150401 (2008).
- [25] J. Perczel, J. Borregaard, D. E. Chang, H. Pichler, S. F. Yelin, P. Zoller, and M. D. Lukin, *Phys. Rev. Lett.* **119**, 023603 (2017).
- [26] A. Grankin, D. V. Vasilyev, P. O. Guimond, B. Vermeresch, and P. Zoller, 1802.05592 (2018).
- [27] D. Barredo, S. De Leseleuc, V. Lienhard, T. Lahaye, and A. Browaeys, *Science* **354**, 1021 (2016).
- [28] M. Endres, H. Bernien, A. Keesling, H. Levine, E. R. Anschuetz, A. Krajenbrink, C. Senko, V. Vuletic, M. Greiner, and M. D. Lukin, *Science* **354**, 1024 (2016).
- [29] Dirk-Sören Lühmann, C. Weitenberg, and K. Sengstock, *Phys. Rev. X* **5**, 031016 (2015).

- [30] S. Ospelkaus, K. K. Ni, D. Wang, M. H. De Miranda, B. Neyenhuis, G. Quémener, P. S. Julienne, J. L. Bohn, D. S. Jin, and J. Ye, *Science* **327**, 853 (2010).
- [31] L. R. Liu, J. D. Hood, Y. Yu, J. T. Zhang, N. R. Hutzler, T. Rosenband, and K. K. Ni, *Science* **903**, 900 (2018).
- [32] K. T. Kapale, in *Prog. Opt.*, Progress in Optics, Vol. 58, edited by E. Wolf (Elsevier, 2013) pp. 199–250.
- [33] K. S. Johnson, J. H. Thywissen, N. H. Dekker, K. K. Berggren, A. P. Chu, R. Younkin, and M. Prentiss, *Science* **280**, 1583 (1998).
- [34] J. E. Thomas, *Opt. Lett.* **14**, 1186 (1989).
- [35] K. D. Stokes, C. Schnurr, R. Gardner, M. Marable, G. Welch, and J. Thomas, *Phys. Rev. Lett.* **67**, 1997 (1991).
- [36] D. Schrader, I. Dotsenko, M. Khudaverdyan, Y. Miroshnychenko, A. Rauschenbeutel, and D. Meschede, *Phys. Rev. Lett.* **93**, 150501 (2004).
- [37] J. R. Gardner, M. L. Marable, G. R. Welch, and J. E. Thomas, *Phys. Rev. Lett.* **70**, 3404 (1993).
- [38] C. Zhang, S. L. Rolston, and S. Das Sarma, *Phys. Rev. A* **74**, 042316 (2006).
- [39] P. J. Lee, M. Anderlini, B. L. Brown, J. Sebby-Strabley, W. D. Phillips, and J. V. Porto, *Phys. Rev. Lett.* **99**, 020402 (2007).
- [40] K. T. Kapale and G. S. Agarwal, *Opt. Lett.* **35**, 2792 (2010).
- [41] F. Le Kien, G. Rempe, W. P. Schleich, and M. S. Zubairy, *Phys. Rev. A* **56**, 2972 (1997).
- [42] S. Qamar, S. Y. Zhu, and M. S. Zubairy, *Phys. Rev. A* **61**, 063806 (2000).
- [43] E. Paspalakis and P. L. Knight, *Phys. Rev. A* **63**, 065802 (2001).
- [44] S. W. Hell, *Science* **316**, 1153 (2007).
- [45] H. Li, V. A. Sautenkov, M. M. Kash, A. V. Sokolov, G. R. Welch, Y. V. Rostovtsev, M. S. Zubairy, and M. O. Scully, *Phys. Rev. A* **78**, 013803 (2008).
- [46] J. Mompert, V. Ahufinger, and G. Birkl, *Phys. Rev. A* **79**, 053638 (2009).
- [47] Q. Sun, M. Al-Amri, M. O. Scully, and M. S. Zubairy, *Phys. Rev. A* **83**, 063818 (2011).
- [48] N. A. Proite, Z. J. Simmons, and D. D. Yavuz, *Phys. Rev. A* **83**, 041803(R) (2011).
- [49] Y. Qi, F. Zhou, T. Huang, Y. Niu, and S. Gong, *J. Mod. Opt.* **59**, 1092 (2012).
- [50] D. Viscor, J. L. Rubio, G. Birkl, J. Mompert, and V. Ahufinger, *Phys. Rev. A* **86**, 063409 (2012).
- [51] D. D. Yavuz and Z. J. Simmons, *Phys. Rev. A* **86**, 013817 (2012).
- [52] J. L. Rubio, D. Viscor, and V. Ahufinger, *Opt. Express* **21**, 022139 (2013).
- [53] Such an intensity profile can be approximately implemented by using existing techniques such as intensity masks [78], Hermite-Gaussian laser modes, or holographic techniques [79].
- [54] “See Supplement for details.”
- [55] Depending on the desired parameters of the trap, choosing a slightly larger detuning δ can sometimes slightly improve the scheme by achieving the optimal trade off between non-adiabaticity and scattering. However, the improvement is insignificant, so we chose to focus on $\delta = \Omega_0^2/\Delta$ to simplify the presentation.
- [56] The transition $^1S_0 - ^3P_2$ has greater matrix element [80] than transition $^1S_0 - ^3P_0$, which makes it possible to work with greater Ω_p .
- [57] The main limitation comes from the off-resonant coupling of $|g\rangle$ by the $\Omega_c(x)$ field to 3P_1 , 3D_2 , and 1P_1 .
- [58] D. Yang, C. Laflamme, D. V. Vasilyev, M. A. Baranov, and P. Zoller, *Phys. Rev. Lett.* **120**, 133601 (2018).
- [59] More precisely, Ω_c couples $|g\rangle = |^1S_0, F = 1/2, m_F = -1/2\rangle$ to $|^3P_1, F = 3/2, m_F = -3/2\rangle$.
- [60] The main limitation comes from the coupling of $|g\rangle$ to the 3P_1 , 3D_2 , and 1P_1 manifolds.
- [61] S. Nascimbene, N. Goldman, N. R. Cooper, and J. Dalibard, *Phys. Rev. Lett.* **115**, 140401 (2015).
- [62] M. A. Cazalilla, A. F. Ho, and M. Ueda, *New J. Phys.* **11**, 103033 (2009).
- [63] A. V. Gorshkov, M. Hermele, V. Gurarie, C. Xu, P. S. Julienne, J. Ye, P. Zoller, E. Demler, M. D. Lukin, and A. M. Rey, *Nat. Phys.* **6**, 289 (2010).
- [64] A. J. Daley, *Quantum Inf. Process.* **10**, 865 (2011).
- [65] M. A. Cazalilla and A. M. Rey, *Reports Prog. Phys.* **77**, 124401 (2014).
- [66] S. Baier, M. J. Mark, D. Petter, K. Aikawa, L. Chomaz, Z. Cai, M. Baranov, P. Zoller, and F. Ferlaino, *Science* **352**, 201 (2016).
- [67] I. Ferrier-Barbut, H. Kadau, M. Schmitt, M. Wenzel, and T. Pfau, *Phys. Rev. Lett.* **116**, 215301 (2016).
- [68] A. de Paz, A. Sharma, A. Chotia, E. Maréchal, J. H. Huckans, P. Pedri, L. Santos, O. Gorceix, L. Vernac, and B. Laburthe-Tolra, *Phys. Rev. Lett.* **111**, 185305 (2013).
- [69] A. Micheli, G. K. Brennen, and P. Zoller, *Nat. Phys.* **2**, 341 (2006).
- [70] M. A. Baranov, *Phys. Rep.* **464**, 71 (2008).
- [71] G. Pupillo, A. Micheli, H. P. Büchler, and P. Zoller, *Cold Mol. Theory, Exp. Appl.* **322**, 421 (2009).
- [72] L. D. Carr, D. DeMille, R. V. Krems, and J. Ye, *New J. Phys.* **11**, 055049 (2009).
- [73] A. V. Gorshkov, S. R. Manmana, G. Chen, J. Ye, E. Demler, M. D. Lukin, and A. M. Rey, *Phys. Rev. Lett.* **107**, 115301 (2011).
- [74] A. V. Gorshkov, S. R. Manmana, G. Chen, E. Demler, M. D. Lukin, and A. M. Rey, *Phys. Rev. A* **84**, 033619 (2011).
- [75] B. Yan, S. A. Moses, B. Gadway, J. P. Covey, K. R. Hazzard, A. M. Rey, D. S. Jin, and J. Ye, *Nature* **501**, 521 (2013).
- [76] J. P. Covey, S. A. Moses, M. Gärttner, A. Safavi-Naini, M. T. Miecnikowski, Z. Fu, J. Schachenmayer, P. S. Julienne, A. M. Rey, D. S. Jin, and J. Ye, *Nat. Commun.* **7**, 24 (2016).
- [77] S. A. Moses, J. P. Covey, M. T. Miecnikowski, B. Yan, B. Gadway, J. Ye, and D. S. Jin, *Science* **350**, 659 (2015).
- [78] S. Eckel, J. G. Lee, F. Jendrzejewski, N. Murray, C. W. Clark, C. J. Lobb, W. D. Phillips, M. Edwards, and G. K. Campbell, *Nature* **506**, 200 (2014).
- [79] A. L. Gaunt, T. F. Schmidutz, I. Gotlibovych, R. P. Smith, and Z. Hadzibabic, *Phys. Rev. Lett.* **110**, 200406 (2013).
- [80] S. G. Porsev and A. Derevianko, *Phys. Rev. A* **69**, 042506 (2004).

I. SUPPLEMENTAL MATERIAL

In Sec. IA, we discuss how to modify the EIT scheme to suppress non-adiabatic corrections. In Sec. IB, we estimate losses to lower dressed states.

A. Modified EIT scheme

Here, we show how to suppress non-adiabatic corrections in the EIT scheme. The idea is that $\Omega_c(0)$ does not necessarily have to go to zero and that the gradient of $\Omega_c(x)$ around $x = w$ can be smaller than for linear $\Omega_c(x) \sim x\Omega_0/\sigma$. Non-adiabatic corrections can then be suppressed by using the following control field [58]: $\Omega_c(x) = \Omega_0(1 + \nu - \cos(kx))$, which does not go to zero as deeply and as sharply as the linear $\Omega_c(x)$.

Expanding $\Omega_c(x)$ around a minimum for $\nu > 0$, we find

$$\Omega_c(x) = \Omega_p(\eta + (x/w)^2), \quad (\text{S1})$$

with $\eta = \nu\Omega_0/\Omega_p$ and $w = \frac{1}{k}\sqrt{2\Omega_p/\Omega_0}$, and which gives rise to

$$V_{\text{tot}} = \frac{\delta_r}{(\eta + (x/w)^2)^2 + 1} + \frac{4E_w(x/w)^2}{((\eta + (x/w)^2)^2 + 1)^2},$$

whose depth can be tuned to accommodate one or more bound states. By operating at $\eta > 0$, we can use appropriate $|\delta_r| \sim E_w$ to engineer trapping potentials with negligible non-adiabatic potential U . Therefore, when it comes to losses, this modified EIT scheme allows us to gain up to a factor of ~ 2 .

B. Landau-Zener estimates of losses to lower dressed states

Another source of losses is tunneling from the single bound state we consider to state $|-\rangle$. Note that, due to the conservation of energy, atoms in $|-\rangle$ will have large kinetic energy. Following [23], the loss rate Γ_{LZ} can be estimated using a Landau-Zener like argument, which, in our setup, leads to

$$\Gamma_{\text{LZ}} \sim E_w e^{-\nu\Delta_{0-}/E_w}, \quad (\text{S2})$$

where ν is a factor of order unity, and Δ_{0-} is the energy difference between two dressed states involved in the tunneling.

In the EIT scheme, we have $\Delta_{0-} \sim |E_-(0)| \sim \Omega_p$ because the tunneling occurs around $x \sim 0$ where the gap between E_D and E_- is smallest and where the atoms are trapped. This leads to the condition $1 \ll \Omega_p/E_w = \Omega_c/(E_\sigma s^3)$. Note that we obtained the same condition from the requirement $E_w \ll \Omega_p$, which enabled us to treat non-adiabatic potentials and light-shifts separately

and perturbatively. We can further suppress tunneling losses by working at $\Delta \neq 0$.

In the blue-detuned AC-Stark scheme, $\Delta_{0-} \sim |E_-| \sim |\Delta|$, so this tunneling loss rate is strongly suppressed as $\exp[-|\Delta|/E_w]$.

In the red-detuned AC-Stark scheme, there is no state below the state of interest and therefore no tunneling.